ISSN 1392–1320 MATERIALS SCIENCE (MEDŽIAGOTYRA). Vol. 25, No. 2. 2019

Process Optimization of Cold Metal Transfer Plug Welding of Aluminum AA6061-T6-to-Galvanized DP590 Steel Based on Orthogonal Experiment Method

Guodong DU, Yanfeng XING *, Chuanya YIN

Shanghai University of Engineering Science, Administrative Building 1016, 333 Longteng Road, Shanghai 201620, China

crossref http://dx.doi.org/10.5755/j01.ms.25.2.18785

Received 09 August 2017; accepted 20 March 2018

In this paper, cold metal transfer (CMT) plug welding of aluminum AA6061-T6-to-galvanized DP590 steel is studied using AlSi-5 welding wire as filler material. The influence of wire feeding speed on welding quality is one of the research emphases. Firstly, an orthogonal experiment is designed to investigate the impact of wire feeding speed, welding speed and arc length correction on the mechanical performance of the joints. In addition, the welding quality of weldments under optimized process parameters are examined by tensile test and metallographic test. Finally, the influence rule of joint shape, metal transition thickness and welding strength under different wire feeding speed is studied. The results show that wire feeding speed has the greatest influence on joint strength. When wire feeding speed goes up from 5.0 m/min to 6.2 m/min, the thickness of intermetallic transition layer increases. The optimal combination of process parameters is analyzed.

Keywords: cold metal transfer, orthogonal experiment, process parameters, wire feeding speed.

1. INTRODUCTION

In order to improve the power performance of the car, reduce fuel consumption and exhaust pollution, lightweight of automobile has become an inevitable development trend of automobile manufacturing [1]. The application of aluminum steel joining structure is one of the important methods to realize the lightweight of automobile body nowadays [2].

However, the differences of physical properties between aluminum and steel are so huge that welding between them is very difficult. Therefore, welding process of aluminum alloy to steel has become a research direction of many scholars. It was possible to produce components in possession of metastable structures using electro- spark welding process [3]. A model based on gene expression programming for predicting impact resistance of aluminum-epoxy laminated composites in both crack divider and crack arrester configurations has been investigated [4]. Friction stir welding was proposed as a technology for joining dissimilar metal and thermoplastics [5]. Zn coating on galvanized steel would be molten under the arc and the evaporation of Zn would lead to extremely high arc pressure and arc instability during arc welding process [6]. Besides arc welding, resistance spot welding has been applied to join aluminum and steel, but the short electrode life was the concern [7, 8]. Analysis of X-ray diffraction results revealed that post-rolling of constrained groove pressed sheets induced dynamic recrystallization due to massive dislocations' accumulation, which is followed by crystallite growth [9]. Compare to gas metal arc welding, Cold Metal Transfer (CMT) welding was widely applied in dissimilar metal welding because of the characteristics of low heat input, free of splashing and strong bridging ability [10]. Coating of the stainless steel with aluminum via common welding methods, including melting processes is very difficult due to difference in their temperature, physical and chemical properties [11]. Therefore, CMT welding technique was introduced as a method to join aluminum to steel [12 – 14]. Researches [15, 16] on CMT welding of aluminum and steel were mainly related to seam welding. It was reported that sound lapped aluminum-bare steel joints could not be produced with CMT method due to the formation of a large amount of the brittle FeAl3 unless reduce the heat input so that the intermetallic could be minimized [17]. Some researchers also investigated the influence of size effects in both micro bulk forming process and micro sheet forming process based on a mixed material model [18, 19].

In order to meet the requirement of varied welding, scholars start to study the method of CMT plug welding of aluminum and steel. They presented that circling the torch along the hole edge can homogenize the heat input to the weld. They also concluded that if weld along the edge of the hole, heat input would be evenly and welding seam

would be good [20]. The results from Cao et al. showed that both weld appearance and joint strength were improved significantly by positioning bare steel with a predrilled hole on the top of aluminum AA6061-T6 [21].

In this paper, orthogonal test method is applied to analyze the influence rule of welding parameters on the joint strength and to screen the optimum process parameter combination. Next, tensile load and metallographic structure of the welds under optimum process parameters are analyzed respectively by stretching machine and electron microscope. Finally, the influence rule of different wire feeding speed on the thickness of metal transition layer, plug joint and welding strength is analyzed.

* Corresponding author. Tel.: +86 21 67791147.
E-mail address: *xyf2001721@163.com* (Y. Xing)

2. EXPERIMENTAL PROCEDURE

2.1. Materials

In this study, the materials used include 1.0 mm thick AA6061-T6 aluminum alloy sheets and 1.0 mm thick galvanized DP590 steel sheets. Welding wire is AlSi-5 with a diameter of 1.2 mm. The chemical compositions of aluminum alloy sheet, welding wire and the galvanized steel sheet are shown in Table 1.

2.2. Sample fabrication

Welding equipment used in this test are Fronius TPS4000 CMT welding machine and KUKA KR5 R1400 robot. The navigation equipped on the machine is RCU5000i controller (Fig. 1). The welding test bed is shown in Fig. 2. The argon with a purity of 99.99 % is used as test gas.

Fig. 1. Welding system

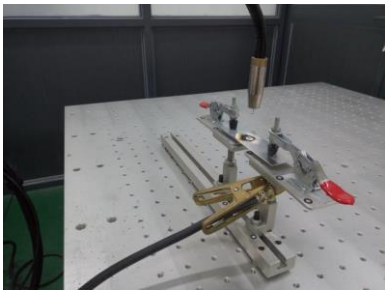

Fig. 2. Welding test rig

The aluminum and steel sheets were cut into coupons having dimensions of 130 mm × 38 mm with an overlap of 50 mm. The aluminum alloy sheet is on top of the steel sheet. The steel sheet has a 7 mm diameter hole located in the center of the overlap. The lap pattern is shown in Fig. 3.

Before welding, specimens are supposed to be cleaned. First, mechanical means were used to remove the oxide film on the surface of aluminum sheets. Then absorbent cotton or fiber sponge was used to scrub the dirt, dust, grease and fingerprints on aluminum and galvanized steel sheets. Finally, acetone was used to clean up dust and blot.

The welding method we adopted is edge plug welding, the welding track is shown in red line in Fig. 4.

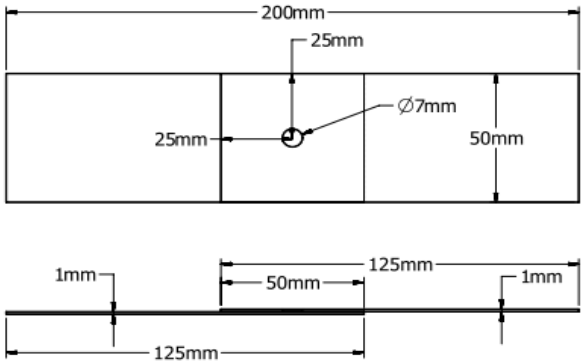

Fig. 3. Schematic of lapped Al-to-steel work piece

The torch remains perpendicular to the aluminum sheet. During welding process, the torch travels around the edge of the hole and the arc is extinguished in the center of the hole at last. The welding method we use can make the heat input more uniform as well as reduce the formation of metal compounds at the plug joints.

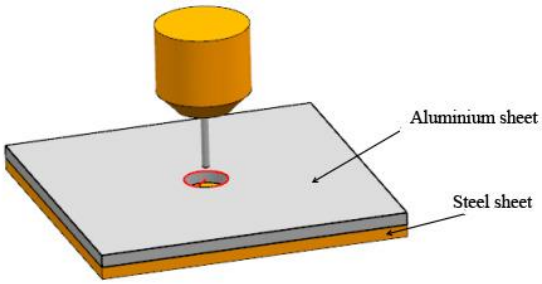

Fig. 4. Schematic of welding mode

2.3. Microstructural analysis

The metallographic samples were cut along the transverse direction of the welding joint. The cross section was grounded, polished and etched. The etchant for etching AA6061 side of samples was mixed by 1 ml HF, 1.5 ml HCL, 2.5 ml HNO_3 and 95 ml H_2O. 4% Nital was used for etching DP590 side. Microstructures of the welding joints under different wire feeding speeds were observed under the optical microscope Leica measuring upright microscope DM4M and scanning electron microscope (SEM) Hitachi S-3400N.

2.4. Mechanical testing

Quasi-static test of each specimen was carried out with a tensile test machine MJDW-200B, which has a maximum experimental force of 200 kN. In order to ensure tensile force through the central axis of the sample, plates of the same thickness were attached to both end of the sample. Results of loading and the corresponding displacement were recorded when specimens were loaded at a stretching rate of 1 mm/min.

Table 1. Chemical compositions of AA6061-T6, ER4043 and DP590, wt.%

Material	Mg	Si	Cu	Mn	Zn	C	Fe	Al
AA6061-T6	0.80 – 1.20	0.40 – 0.80	0.15 – 0.40	0.15	0.25	0.25	0.70	Bal.
ER4043	0.05	4.5 – 6.0	0.30	0.05	0.10	–	0.80	Bal.
DP590	–	< 0.80	–	< 2.20	–	< 0.18	Bal.	–

Each group of tests was repeated three times, and the peak load we adopted is the average of the three test results.

3. RESULTS AND DISCUSSION

3.1. The optimal process parameters of plug welding of AA6061-T6 to galvanized DP590

The welding parameters, which influence the quality of welding joints, include the distance between the end of welding torch and the weldment (gun distance), dry elongation, welding speed, wire feeding speed, arc length correction, gas flow and protection time, etc. Welding current and welding voltage size are determined by wire feeding speed directly. Welding current and welding voltage determine the heat input Q which can be calculated from Eq. 1 precisely [22]:

$$Q = \frac{\eta \times V \times I \times 60}{S \times 1000}, \quad (1)$$

where V is the arc voltage in volts, I is the arc current in amperes, S is the welding speed in mm/min and $\eta = 0.8$ is the arc efficiency.

The function of arc length correction is used to automatically adjust the arc length through the digital circuit system during welding. Welding speed directly affects the welding time. Softening phenomena of AA6061-T6 will occur during welding process if weld torch is positioned too close to the weld root. The mechanical strength of AA6061-T6 will decrease [23]. Therefore, it is supposed to control the torch deviation distance at 2 mm for CMT welding. This paper mainly analyzed the influence of these three process parameters on the quality of CMT spot welding joint. The orthogonal test was adopted to optimize the CMT joining process parameters. Wire speed, welding speed and arc length correction were selected as the three factors of orthogonal test, each factor employs three levels. Welding test factor levels are shown in Table 2.

Table 2. Experimental factors and levels

No.	Factor A Wire feed speed, m/min	Factor B Welding speed, m/min	Factor C Arc length orrection
1	5	1.2	15
2	5.6	1.5	0
3	6	1.8	– 15

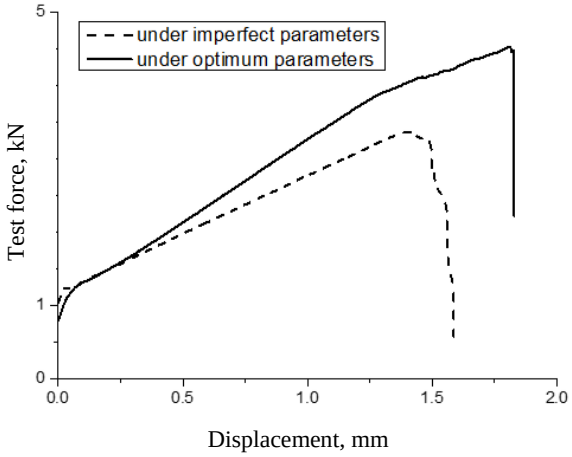

Fig. 5. Test force and tensile deformation displacement curve

Table 3. Input parameters of the orthogonal array and output characteristics

No	A (wire feeding speed, m/min	B (welding speed, m/min	C (arc length correction)	Peak load, kN
1	5	1.2	15	3.18
2	5	1.5	0	3.37
3	5	1.8	– 15	3.07
4	5.6	1.2	0	4.53
5	5.6	1.5	– 15	3.85
6	5.6	1.8	15	3.68
7	6.0	1.2	– 15	2.93
8	6.0	1.5	15	3.74
9	6.0	1.8	0	3.63

Orthogonal test values are shown in Table 3. The evaluation criteria are the peak load of the weldment. Rank analysis of process parameters is presented in Table 4. The range of wire feeding speed is 0.81, the range of welding speed is 0.19, and the range of arc length correction is 0.56. The sequential order of process parameters that influence the welding strength is wire feeding speed, arc length correction and welding speed. The optimal parameter of welding is that the wire feed speed is 5.6 m/min, the welding speed is 1.2 m/s, and the arc length correction is 0. The tensile strength of the weldment under the optimal process parameters is the largest one.

Table 4. Experimental results of rank analysis

Factor	A	B	C
K_1	9.62	10.96	10.60
K_2	12.05	10.82	11.52
K_3	10.30	10.38	9.85
k_1	3.21	3.65	3.53
k_2	4.02	3.61	3.84
k_3	3.43	3.46	3.28
Range	0.81	0.19	0.56
Rank	A > C > B		
Optimal level combination	$A_2B_1C_2$		

3.2. Analysis of optimized AA6061-T6 to galvanized steel

The mechanical and metallographic analysis of the weldment under the optimum and imperfect parameters were carried out. The change curve of test force with tensile displacement is shown in Fig. 5. It can be seen from Fig. 5 that the elastic deformation occurs first under the action of tensile force and then the plastic deformation occurs. It can judge from Fig. 5 that the mechanical performance of the weldment under optimum parameters is better than that under imperfect parameters. It can be investigated from Fig. 6 that the steel sheet is not distortion and the aluminum sheet is distorted at the plug joint. It can be deduced from the drawing that the plastic deformation is caused by aluminum sheet.

The shape of plug joint is shown in Fig. 7. It can be seen in Fig. 7 a that the weld appearance is good, molten wire is evenly covered around the hole on the aluminum sheet, and

aluminum plate is not melted through. The droplet is fused together with the aluminum plate. At the same time, the droplet passes through the small hole and is well brazed with the galvanized steel sheet, and the welding quality is good. Moreover, molten aluminum alloys have a high affinity for zinc which is the basis for improved wetting of the filler material to zinc-coated steels [24]. As shown in Fig. 7 b, the galvanized layer of steel plate and the fuse are evaporated, leaving a light black area, and the color of the area is dark. From the cross-section diagram Fig. 7 c and d, it can be seen that region 1 corresponds to a region where evaporation color is darker and region 2 corresponds to a region where the color of the evaporation is lighter. It can be concluded that heat input in region 1 is higher than that in region 2. In the meantime, the weld joint tearing in region 1 instead of region 2 during the tensile shear test.

Fig. 8 a is a metallographic structure chart of the cross-section of aluminum-steel welded joint. It can be seen from Fig. 8 a that there is a metal transition layer between aluminum and steel. SEM image at region 1 in Fig. 8 a is shown in Fig. 8 b, which shows that the maximum metal transition layer thickness is 6.25 μm. Table 5 gives the results of energy spectrum analysis of region a and b in Fig. 7. The ratio of Fe atoms to Al atoms at region a is close to 1:3, from which we can infer that it is $FeAl_3$. $FeAl_3$ is needle-like in shape. There exist two main reasons for the formation of $FeAl_3$: one is the thermal conductivity of aluminum is better than that of steel, the other is the negative temperature gradient is formed at the interface so that the growth of $FeAl_3$ crystal is faster [25]. The ratio of Fe atoms to Al atoms at point b is close to 1:2.5, from which we can infer that it is Fe_2Al_5. It can be observed in Fig. 8 b that the transition layer near the aluminum side is uneven, and the transition layer is relatively smooth near the side of the steel. The reason for this phenomenon is that the compound $FeAl_3$ produced on the side of the aluminum sheet is rendered as a long needle.

a b

Fig. 6. Steel sheet and aluminum sheet after tensile load test: a – steel sheet; b – aluminum sheet

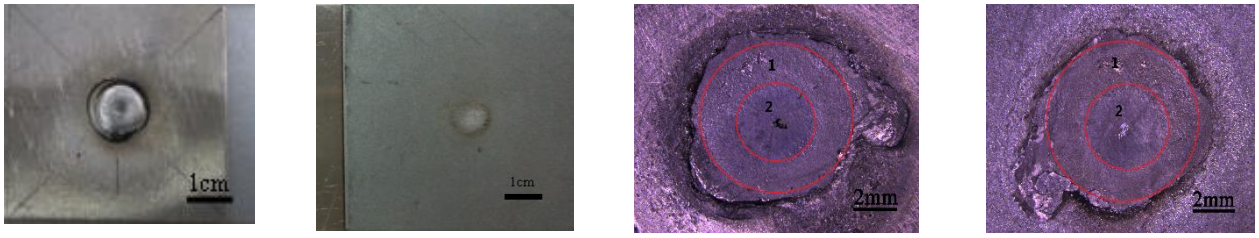

a b c d

Fig. 7. Shape of welding spot and tensile failure section, region 1 corresponds to a region where evaporation color is darker, region 2 corresponds to a region where the color of the evaporation is lighter: a – frontage of plug joint; b – back of plug joint; c – aluminum plate welding section; d – steel plate welding section

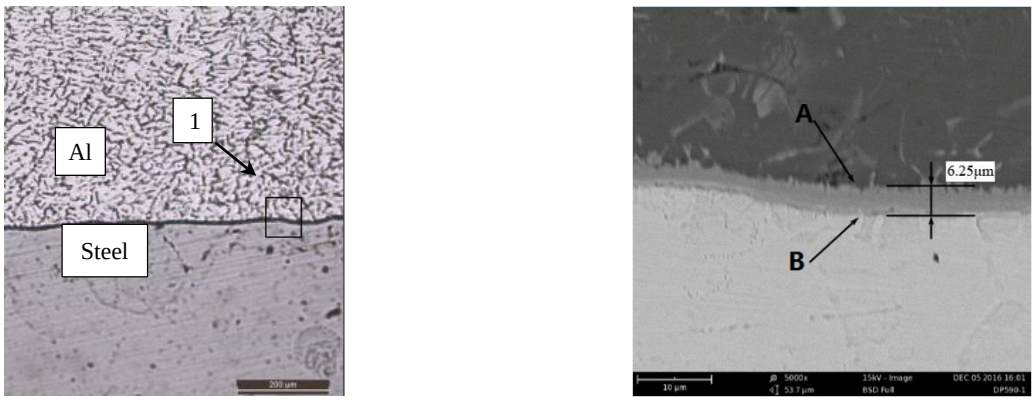

a b

Fig. 8. Microstructures of CMT plug weld in optimal process, region 1 in a is a part of metal transition layer and its SEM result is shown in b

Table. 5. Compositions of positions in Fig. 8 atom fraction, %

	Fe	Al	Si	Zn
A	22.1	76.2	1.2	0.5
B	27.2	68.9	2.8	1.1

3.3. The influence rule of wire feeding speed on plug welding

The analysis of orthogonal test result shows that wire feeding speed has great influence on the joint strength of welded joints. In this section, the influence of different wire feeding speeds on the joint strength and the appearance of plug joints is analyzed. Taking welding speed of 1.2 m/min and arc length correction 0 as the invariable condition, four different feeding speeds (5 m/min, 5.4 m/min, 5.8 m/min and 6.2 m/min) were selected to carry out welding experiments. The shape of the plug joints at four wire feed speed is shown in Fig. 9. It can be seen from the figure that as wire feeding speed rises, the degree of burning on the surface of aluminum sheet gradually increases, on account of the aluminum has lower melting point and is more sensitive to heat. With the escalation of wire feeding speed, the welding current and voltage increase continuously, so that the welding heat input rises, causing the loss of aluminum sheet increases continuously.

The thickness of intermetallic transition layer under different wire feeding speed is shown in Fig. 10. It can be seen from Fig. 10 that the thickness of metal transition layer increases as wire feeding speed increases. Moreover, since wire feeding speed determines the heat input directly, so that welding heat input has a direct influence on the thickness of metal transition layer. It can be seen from Fig. 11 that the height of plug joint decreases slowly with the escalation of wire feeding speed, while the diameter of plug joint appears on the contrary. This is because with the augmentation of wire feeding speed, welding heat input increased. While the amount of wire is also increasing, so the aluminum nugget expands, the droplet spreading on the aluminum plate is more open, the plug joint diameter enlarges, the plug joint height decrease slowly. Tensile tests were carried out on the four sets of specimens and the results show that the welded joints were all fractured from the transition layer of aluminum-steel. The joint strength and the thickness of the transition layer are shown in Fig. 11. The tensile load of the weldment grows with the increase of the wire feeding speed. When wire feeding speed is 5.8 m/min, the tensile load reaches 4.21 KN, but the tensile load decreases to 2.74 KN when wire feeding speed reaches 6.2 m/min. It can be seen from the figure that tensile load rises with the increase of the thickness of the metal transition layer, but when the thickness of metal transition layer exceeds 10 μm to 16.71 μm, the tensile load drops sharply. It was analyzed that when the thickness of metal compound (transition layer) formed by the connection of the aluminum steel was no more than 10 μm, the connection quality of the aluminum steel was fine [26]. Moreover, combined with this section we can see that aluminum alloy welding strength is not ideal if the thickness of the transition layer is too small or too large, that is, if you want to ensure the strength of aluminum welding, the metal transition layer thickness must be maintained within the appropriate range.

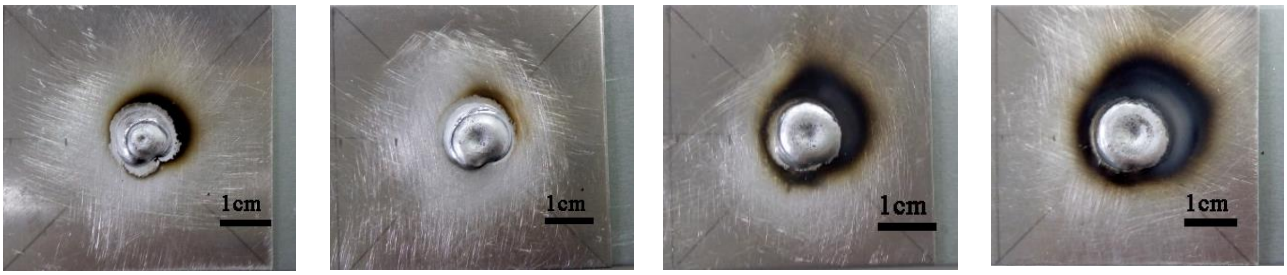

a b c d

Fig. 9. The plug joint shape by four kinds of wire feed speed: a – wire feeding speed 5.0 m/min; b – wire feeding speed 5.4 m/min; c – wire feeding speed 5.8 m/min; d – wire feeding speed 6.2 m/min

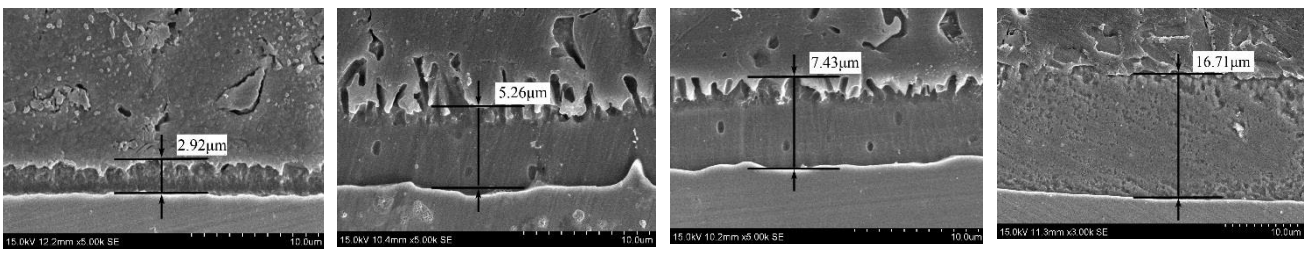

a b c d

Fig. 10. SEM images of IMC layer: a – wire feeding speed 5.0 m/min; b – wire feeding speed 5.4 m/min; c – wire feeding speed 5.8 m/min; d – wire feeding speed 6.2 m/min

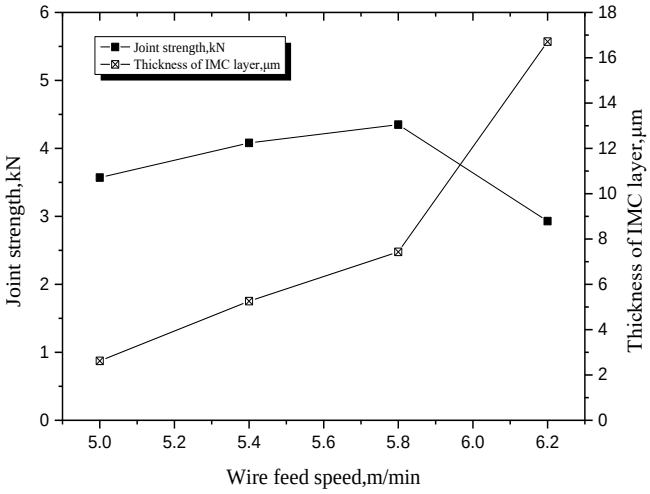

a

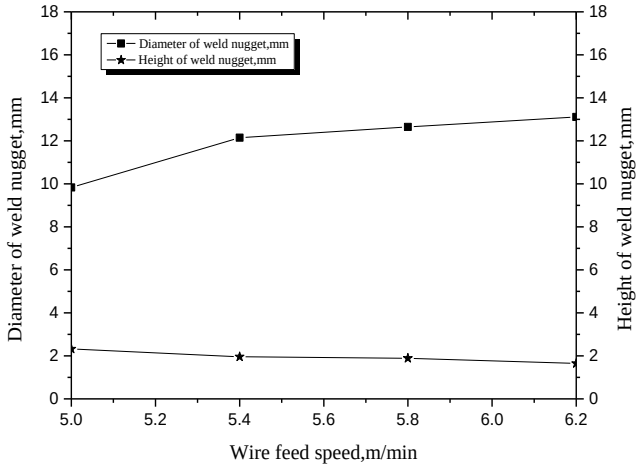

b

Fig. 11. Effect of wire feed speed: a – effect of wire feed speed on joint strength and IMC layer thickness; b – effect of wire feed speed on nugget diameter and nugget height

4. CONCLUSIONS

Orthogonal test method was applied in this paper to analyze the influence rule of welding parameters on the joint strength and to screen the optimum process parameter combination. The contributions of this paper are:

1. Orthogonal test results reveal that wire feeding speed has the greatest influence on the connection strength, arc length is the second, and the welding speed has the least influence. The optimum combination of process parameters is wire feed speed 5.6 m/min, welding speed 1.2 m/s, arc length correction 0.
2. When welding experiment is carried out with the optimum scheme, the droplet is uniformly covered on the aluminum sheet and better spread out on the galvanized steel sheet. The tensile load of weldment reaches 4.53 kN. The transition layer of welded joint close to aluminum sheet is mainly composed of $FeAl_3$, while the metal compound near the steel sheet is mainly Fe_2Al_5.
3. When wire feeding speed rises from 5 m/min to 6.2 m/min, the welding heat input increases continuously, the thickness of the metal transition layer increases gradually, and the connection strength of the weldment is enhanced as well. However, when heat input adds up to a certain value, the connection strength decrease. As heat input increases, the nugget becomes larger and the droplet spreads more openly on the weld, which enlarges the diameter of plug point, while the solder height goes down slowly.

Acknowledgments

This work was financially supported by National Natural Science Foundation of China (51575335). This work was financially supported by "Shuguang Program" supported by Shanghai Education Development Foundation and Shanghai Municipal Education Commission (16SG48). This work was financially supported by Science and Technology Commission of Shanghai Municipality (16030501300).

REFERENCES

1. **Naderia, M., Ketabchi, M., Abbasi, M., Bleck, W.** Analysis of Microstructure and Mechanical Properties of Different High Strength Carbon Steels after Hot Stamping *Journal of Materials Processing Technology* 211 (6) 2011: pp. 1117 – 1125. https://doi.org/10.1016/j.jmatprotec.2011.01.015
2. **Hansen, S.R., Vivek, A., Daehn, G.S.** Impact Welding of Aluminum Alloys 6061 and 5052 by Vaporizing Foil Actuators: Heat-affected Zone Size and Peel Strength *Journal of Manufacturing Science and Engineering* 137 (5) 2015: pp. 051013. https://doi.org/10.1115/1.4030934
3. **Brochu, M., Heard, D.W., Milligan, J., Cadney, S.** Bulk Nanostructure and Amorphous Metallic Components Using the Electro Spark Welding Process *Assembly Automation* 30 (3) 2010: pp. 248 – 256. https://doi.org/10.1108/01445151011061145
4. **Nazari, A., Khalaj, G., Didehvar, N.** Computational Investigations of the Impact Resistance of Aluminum–Epoxy–Laminated Composites *International Journal of Damage Mechanics* 21 (5) 2012: pp. 623 – 646. https://doi.org/10.1177/1056789511411739
5. **Bozkurt, Y., Kentli, A., Uzun, H., Salman, S.** Experimental Investigation and Prediction of Mechanical Properties of Friction Stir Welded Aluminum Metal Matrix Composite Plates *Materials Science (Medziagotyra)* 18 (4) 2012: pp. 336 – 340. https://doi.org/10.5755/j01.ms.18.4.3092
6. **Rao, Z., Liu, J., Wang, P.C., Li, Y., Liao, S.** Modeling of Cold Metal Transfer Spot Welding of AA6061-T6 Aluminum Alloy and Galvanized Mild Steel *Journal of Manufacturing Science and Engineering* 136 (5) 2014: pp. 051001. https://doi.org/10.1115/1.4027673
7. **Bakavos, D., Prangnell, P.B.** Effect of Reduced or Zero Pin Length and Anvil Insulation on Friction Stir Spot Welding Thin Gauge 6111 Automotive Sheet *Science and Technology of Welding and Joining* 14 (5) 2009: pp. 443 – 456. https://doi.org/10.1179/136217109x427494
8. **Peng, J., Fukumoto, S., Brow, L., Zhou, N.** Image Analysis of Electrode Degradation in Resistance Spot Welding of Aluminum *Science and Technology of Welding and Joining* 9 (4) 2004: pp. 331 – 336. https://doi.org/10.1179/136217104225012256

9. **Jandaghi, M.R., Pouraliakbar, H., Khalaj, G., Khalaj, M.J., Heidarzadeh, A.** Study on the Post-Rolling Direction of Severely Plastic Deformed Aluminum-Manganese-Silicon Alloy *Archives of Civil and Mechanical Engineering* 16 (4) 2016: pp. 876 – 887. https://doi.org/10.1016/j.acme.2016.06.005
10. **Pickin, C.G., Young, K.** Evaluation of Cold Metal Transfer (CMT) Process for Welding Aluminum Alloy *Science and Technology of Welding and Joining* 11 (5) 2006: pp. 583 – 585. https://doi.org/10.1179/174329306x120886
11. **Mohammad Reza Khanzadeh Ghareh, S., Haimd, B., Seyed Ali-Asghar Akbari, M., Gholamreza, K., Seyed Majid, M.** Effect of Stand-Off Distance on the Mechanical and Metallurgical Properties of Explosively Bonded 321 Austenitic Stainless Steel – 1230 Aluminum Alloy Tubes *Materials Research* 20 (2) 2017: pp. 291 – 302. https://doi.org/10.1590/1980-5373-mr-2016-0516
12. **Yang, X.R.** Cold Metal Transfer MIG/MAG Dip-Transfer Process for Automated Applications *Electric Welding Machine* 36 (6) 2006: pp. 5 – 7 (in Chinese). https://doi.org/10.3969/j.issn.1001-2303.2006.06.003
13. **Yang, S., Zhang, J., Lian, J., Lei, Y.** Welding of Aluminum Alloy to Zinc Coated Steel by Cold Metal Transfer *Materials and Design* 49 2013: pp. 602 – 612. https://doi.org/10.1016/j.matdes.2013.01.045
14. **Cao, R., Yu, G., Chen, J.H., Wang, P.C.** Cold Metal Transfer Joining Aluminum Alloys-to-Galvanized Mild Steel *Journal of Materials Processing Tech* 213 (10) 2013: pp. 1753 – 1763. https://doi.org/10.1016/j.matdes.2013.01.045
15. **Zhang, H.T., Feng, J.C., He, P.** Interfacial Phenomena of Cold Metal Transfer (CMT) Welding of Zinc Coated Steel and Wrought Aluminum *Materials Science and Technology* 24 (11) 2008: pp. 1346 – 1349. https://doi.org/10.1179/174328407x213152
16. **Kobayashi, S., Yakou, T.** Control of Intermetallic Compound Layers at Interface between Steel and Aluminum by Diffusion-treatment *Materials Science and Engineering A* 338 (1 – 2) 2002: pp. 44 – 53. https://doi.org/10.1016/s0921-5093(02)00053-9
17. **Cao, R., Sun, J.H., Chen, J.H., Wang, P.C.** Cold Metal Transfer Joining of Aluminum AA6061-T6-to-Galvanized Boron Steel *Journal of Manufacturing Science and Engineering* 136(5) 2014: pp. 051015. https://doi.org/10.1115/1.4028012
18. **Lai, X.M, Peng, L.F, Hu, P., Lan, S.** Material Behavior Modelling in Micro/Meso-Scale Forming Process with Considering Size/Scale Effects *Computational Materials Science* 43 (4) 2008: pp. 1003 – 1009. https://doi.org/10.1016/j.commatsci.2008.02.017
19. **Peng, L.F, Lai, X.M, Lee, H.J., Song, J.H.** Analysis of Micro/Mesoscale Sheet Forming Process with Uniform Size Dependent Material Constitutive Model *Materials Science and Engineering A* 526 (1 – 2) 2009: pp. 93 – 99. https://doi.org/10.1016/j.msea.2009.06.061
20. **Lei, H., Li, Y., Carlson, B.E., Lin, Z.** Microstructure and Mechanical Performance of CMT Spot Joints of AA6061-T6 to Galvanized DP590 Using Edge Plug Welding Mode *Journal of Manufacturing Science and Engineering* 138 (7) 2015: pp. 071009. https://doi.org/10.1115/1.4032082
21. **Cao, R., Huang, Q., Zeng, C.Z., Ai, B.Q., Lin, Q., Wang, P.Ch.** Cold Metal Transfer Plug Welding of Aluminum AA6061-T6-to-Bare Mild Steel *Journal of Manufacturing Science and Engineering* 138 (8) 2016: pp. 081008. https://doi.org/10.1115/1.4033040
22. **Madhavan, S., Kamaraj, M., Vijayaraghavan, L., Rao, K.S.** Cold Metal Transfer Welding of Dissimilar A6061 Aluminum Alloy-AZ31B Magnesium Alloy: Effect of Heat Input on Microstructure, Residual Stress and Corrosion Behavior *Transactions of the Indian Institute of Metals* 70 (4) 2016: pp. 1 – 8. https://doi.org/10.1007/s12666-016-0893-9
23. **Cao, R., Sun, J.H., Chen, J.H.** Mechanisms of Joining Aluminum A6061-T6 and Titanium Ti-6Al-4V Alloys by Cold Metal Transfer Technology *Science and Technology of Welding and Joining* 18 (5) 2013: pp. 425 – 433. https://doi.org/10.1179/1362171813y.0000000118
24. **Okamoto, H.** A1-Zn (Aluminum-Zinc) *Journal of Phase Equilibria* 16 (3) 1995: pp. 281 – 282. https://doi.org/10.1007/bf02667316
25. **Guo, X., Zhao, Y., He, T. Q.** Study on Microstructure and Mechanical Property of Welding-brazing Joints of Aluminum Alloy to Galvanized Steel by CMT *Hot Working Technology* 44 (23) 2015: pp. 231 – 233 (in Chinese). https://doi.org/10.14158/j.cnki.1001-3814.2015.23.068
26. **Schubert, E., Klassen, M., Zerner, I.** Light-Weight Structures Produced by Laser Beam Joining for Future Applications in Automobile and Aerospace Industry *Journal of Materials Processing Tech* 115 (1) 2001: pp. 2 – 8. https://doi.org/10.1016/s0924-0136(01)00756-7